Virtual enhancement of marker X-ray visibility for cerebral stents and flow diverters

Manthey S.[1], Hoffmann T.[2], Cattaneo G[3]., Beuing O[2], Preim B.[1], Saalfeld S.[2]

[1]OvG-University, Department of Simulation and Graphics, Magdeburg, Germany
[2]OvG-University, Institute of Neuroradiology, Magdeburg, Germany
[3]Acandis GmbH & Co KG, Pforzheim, Germany

Kontakt: samuel.manthey@ovgu.de

Abstract

Stents are common devices for endovascular X-ray-guided treatment of neurovascular diseases like aneurysms or artherosclerosis, but their visibility may be hampered in clinical practice. To improve visibility during interventions, they are equipped with radiopaque markers. However, since the marker size is limited, stents may still be nearly invisible during deployment. Therefore, we virtually enhanced these markers with an overlay supplied by a detection algorithm. For validation, eight data sets were acquired with a skull phantom and different stents in an angiography suite. Subsequently, a physician compared the enhanced and the unaltered images qualitatively. In addition, first results for clinical images are presented. It was successfully demonstrated that the visibility of X-ray markers can be increased with image-based techniques. Furthermore, the markers of current devices are of sufficient size and opacity to be detected by feature detectors. In future, the image-based detection of X-ray markers may assist in precise stent deployment.

Keywords: stent, flow diverter, stent enhancement, marker detection, X-ray marker, X-ray visibility, image processing

1 Problem

Stents and flow diverters are tubular meshed devices for treating different endovascular diseases for example aneurysms, stenosis or atherosclerotic vessels. In order to estimate the beginning and the end of such devices in X-ray images, they are equipped with radio-opaque markers at these points. Through limitations in size and material, those markers can still be hard to recognize, therefore virtual enhancement seems like a natural choice to assist during device deployment. The methods for detecting and enhancing devices in X-ray images have mainly been developed for interventions and device deployment in the thorax. In [3] and [4] the authors use different blob detectors for identifying catheters during cardiac electrophysiology interventions. Here, the focus lays more on detecting and tracking of those markers then on marker enhancement, since the markers of thorax catheters are large and well recognisable. A similar approach is used in [2] for the detection of guide wire markers for cardiac stents. This method is called digital stent enhancement (DSE). Here the markers are tracked over multiple images during the motion of the heart. With the marker locations, consecutive images are registered onto each other and averaged. In the averaged images the stent can be seen more clearly. This method is very popular and has been improved over the last years for example by [1] and is even used commercially. Since DSE was specifically designed for the cardiac stents, we propose a method suitable for the cerebral application. Its main goal is to detect and to enhance the X-ray markers of cerebral stents and flow diverters. Figure 1 A shows a stent half deployed in a skull phantom as an example for a detection task.

2 Material and Methods

This section starts with an overview of the marker detection, followed by describing the acquisition of the phantom images and closes with an explanation of the evaluation of the results.

2.1 Marker Detection and Enhancement

The proposed method for detecting markers is divided into three steps: image pre-processing, marker candidate detection and candidate examination.

2.1.1 Image Pre-Processing

Inputs for the following algorithm are two X-ray projection images: a native reference image of the patient without stent and an image with stent. First, the reference image is subtracted from the current image in order to reduce interference of bones and markers.

The intensity values (J) of an X-ray image are the result of the absorption of radiation by the matter between the X-ray source and the image detector. This process can be described by the Beer-Lambert law with respect to the initial intensity before radiation is absorbed (J_0), the absorption coefficients (μ_i) for all materials the radiation passes through and their respective thickness (D_i):

$$J = J_0 e^{-\sum \mu_i D_i} \qquad (1)$$

The pixel intensity of the reference image depends on the attenuation properties of the transmitted material. The attenuation is expressed by the averaged absorption coefficient (μ_R) over the full thickness of the patient (D_R). The following formula refers to the intensities (J_R) of the reference image with the initial intensity (J_0).

$$J_R = J_0 e^{-\mu_R D_R} \qquad (2)$$

The intensity values of the current image (J_C) additionally depend on the absorption coefficient (μ_C) and thickness of the devices (D_C):

$$J_C = J_0 e^{-(\mu_R (D_R - D_C) + \mu_C D_C)} \qquad (3)$$

In order to obtain an image that only relays on the absorption caused by the devices, the intensities of both images are logarithmized and then subtracted. With the assumption that the absorption coefficient of typical stent marker materials (e.g. gold, platinum) of the devices is different than the coefficient of the replaced volume element of tissue by the marker ($\mu_C \neq \mu_R$) it follows that:

$$ln(J_c) - ln(J_R) = ln(J_0) - (\mu_R (D_R - D_C) + \mu_C D_c)$$
$$- ln(J_0) - \mu_R D_R = D_c(\mu_R - \mu_C) \qquad (4)$$

The equation shows that the pixel intensity in the subtracted image is only different from zero when changes occur in the current image with respect to the reference image. Figure 1 B illustrates the result of the subtraction for the same case as in Figure 1 A. However, such results can be only achieved if reference image and current image perfectly concur. Thus, the subtraction is carried out in the same way as for digital subtraction angiography.

2.1.2 Marker Candidate Detection

After the markers have been emphasised through subtraction of the reference image, candidate regions are determined. Due to the blob-like appearance of the sought regions, a Laplacian of Gaussian (LoG) blob detector is used. This detector works by convolving the subtracted Image (I_S) with a LoG kernel ($LoG(x, y, t)$) and supplying the detector response (R_{LoG}).

$$R_{LoG} = LoG(x, y, t) * R_{LoG} \qquad (5)$$

The LoG kernel is defined by the following equation requiring the voxel coordinates (x, y) and the scale (t).

$$LoG(x, y, t) = \frac{1}{\pi t^2}\left[\frac{x^2+y^2}{2t} - 1\right] e^{-\frac{x^2+y^2}{2t}} \qquad (6)$$

The scale controls for which blob size (number of pixels) the detector delivers the highest response and has to be selected according to the size of the markers to be detected. The pixel number is highly dependent on the cone beam geometry of the X-ray system. Thus, a magnification factor has to be considered for setting the scale. A threshold is applied to the detector response in order to find regions with correspondence to marker candidates. A suitable threshold (θ) is calculated with regards to the mean (μ_{LoG}), standard deviation (s_{LoG}) of the response image and the parameter α.

$$\theta = \mu_{LoG} + \alpha s_{LoG} \qquad (7)$$

The parameter α was empirically determined as $\alpha = 4.4$. The thresholding yields a binary image (T_{BW}) containing a set of n connected regions which are the candidates (C_i) for marker positions.

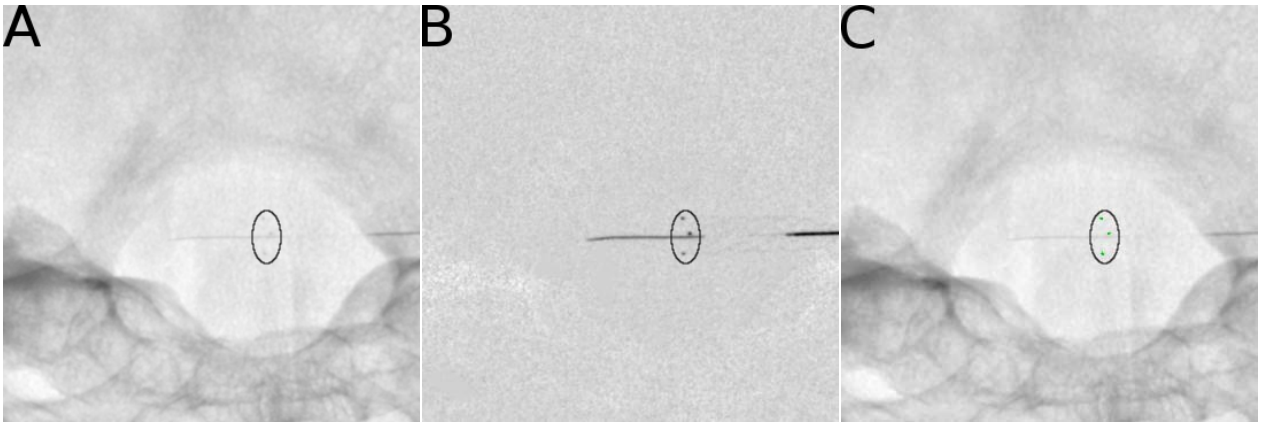

Figure 1: A: Original image with stent marker indicated by the black ellipse and guide wire, B: Same image after subtraction of reference image with stent marker indicated by the black ellipse, C: Image with detected markers indicated by overlay in black ellipse

2.1.3 Candidate Examination

In order to reduce the number of false positives, two different properties of candidates are examined. The first property is the area of a candidate (A_{C_i}). If the area is smaller than a minimum area (A_{min}) or larger than a maximum (A_{max}) all pixels in T_{BW} belonging to C_i are set to zero;

$$T_{BW}(C_i) = 0 \; \forall \left\{ C_i | \, A_{C_i} > A_{max} \;\; \vee \;\; A_{C_i} < A_{min} \right\} \qquad (8)$$

The minimum and maximum areas have to be calculated from the size of the searched markers, the magnification factor and the image pixel spacing of the detector. In a second step, all remaining candidates are checked for their eccentricity. The eccentricity (E_{C_i}) is a measure of the roundness of a candidate, it adapts values between 0 (perfect circle) and 1 (perfect line segment). In this case the implementation in MATLAB® 2016b (Mathworks, USA) is used, where the eccentricity is the ratio of the difference between the foci of the ellipse and the major axis of the ellipse and its major axis. The threshold for E_{C_i} that determines which candidate C_i is deleted has to be extracted based on the geometry of the desired markers. This measure is more useful for markers with a spherical shape but it can still be used on cylindrical markers, for example to distinguish them from false positives caused by guide wires.

2.2 Image Acquisition

A human skull preparation was placed on top of a 150mm thick polymethyl methacrylate scattering body for mimicking human attenuation properties. Two stents, ACCLINO flex (ACANDIS GmbH & Co. KG, Pforzheim, Germany) and Enterprise (Codman Neuro, Raynham, USA), were placed between scattering body and skull after reference image acquisition. Imaging was done with a Siemens Artis zeego angiography system (Siemens Healthineers GmbH, Erlangen, Germany) at 70 kV in radiographic mode. Eight phantom data sets in different orientations were acquired. A clinical radiography data set of a patient treated with a DERIVO (ACANDIS GmbH & Co. KG, Pforzheim, Germany) flow diverter stent was used for a first test under clinical conditions (see Figure 2).

2.3 Clinical Evaluation

The resulting images were compared to the data sets without marker enhancement and qualitatively assessed by an experienced neuroradiologist.

3 Results

In this section, the results of the marker detection applied to the phantom cases are summarized. Table 1 provides an overview of detected markers. The third and fourth columns of Table 1 show how many markers the specific image contained and how many of those were detected. The last two columns indicate if a stent was visible to the physician before and after enhancement.

Table 1: Results for marker detection and enhancement for phantom cases

Nr.:	Device	Markers present	Markers detected	Visible before	Visible after
1	Acclino	3	3	No	Yes
2	Enterprise	4	3	No	Yes
3	Acclino	3	2	Yes	Yes
4	Enterprise	4	2	Yes	Yes
5	Enterprise	4	4	No	Yes
6	Acclino	3	3	Yes	Yes
7	Enterprise	4	4	Yes	Yes
8	Acclino, Enterprise	7	7	Yes	Yes

With the exception of images Nr. 2, 3 and 4, all markers were detected correctly. However, in image 4, the markers of the stent seemed to be rotated in such a way that two markers superimposed each other. In all images, false positive responses were present. Figure 1 C shows the result for the image depicted in Figure 1 A. In this specific segment, no false positives emerged. Columns 5 and 6 of Table 1 depict in which images an improvement of visibility was achieved under the assessment of a physician. In the images Nr. 1, 2 and 5, the markers were occluded by bone prior to the enhancement.

4 Discussion

Although the proposed method was able to detect most markers in the phantom caeses, it relies on the subtraction of a reference frame which is assumed to be perfectly aligned with the current frame. Although this assumption holds for the used phantom images it is certainly unacceptable in the clinical day-to-day life. In the future this problem could be approached with an automatic registration of the reference image on the current image. Another possible improvement would be to incorporate information from a second set of X-Ray images of the same scene taken from different angle in order to acquire spatial information. Finally, Figure 2 displays a first result achieved with our method on a clinical image taken during flow diverter deployment. Although false positives are present in this image all markers of the flow diverter were detected as well as the two markers of the catheter. The image is a promising result for future work.

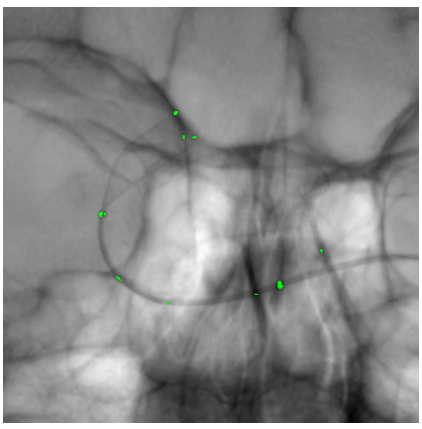

Figure 2: Clinical image with detected markers of a flow diverter and the catheter

5 Conclusion

This study is a summary of early results for a feature-based cerebral stent marker enhancement method. To emphasize markers in regions with dense bone, we first subtracted a reference frame from the current frame. In order to find marker like regions, we used a feature detector according to the expacted appearance in radiographic images. After detection the number of false positives was reduced by comparing each region with maker specific properties. For validation, eight data sets were acquired with a skull phantom and different stents in an angio lab. Subsequently, a physician compared the enhanced and the unaltered images qualitatively. For the small group of phantom images, the method delivered reliable results. In the three cases were the markers were not visible before enhancement to the physician the proposed method restored visibility. It was also shown that the markers currently used on devices are big enough to be detected by simple feature detectors.

Acknowledgment

The work of this paper was partly funded by the Federal Ministry of Education and Research within the Forschungscampus *STIMULATE* under grant number '13GW0095A' and '13GW0095F'.

Author's Statement

Research funding: Conflict of interest: Giorgio Cattaneo is employed in Acandis GmbH, which provided test material, other authors state no conflict of interest. Informed consent: Informed consent has been obtained from all individuals included in this study. Ethical approval: The research related to human use complies with all the relevant national regulations, institutional policies and was performed in accordance with the tenets of the Helsinki Declaration, and has been approved by the authors' institutional review board or equivalent committee.

References

[1] Bismuth V, Vaillant R, Funck F, Guillard N, Najman L. A comprehensive study of stent visualization enhancement in X-ray images by image processing means., Med Image Anal, 2011 Aug;15(4):565-76

[2] Close R. A., Abbey C. K., Whiting J. S., Improved image guidance of coronary stent deployment. Proc. SPIE 3976, Medical Imaging 2000: Image Display and Visualization, 301 (April 18, 2000);

[3] Ma Y, Gogin N, Cathier P, Housden RJ, Gijsbers G, Cooklin M, O'Neill M, Gill J, Rinaldi CA, Razavi R, Rhode KS Real-time x-ray fluoroscopy-based catheter detection and tracking for cardiac electrophysiology interventions., Med Phys. 2013;40(7):071902

[4] Ma Y, King AP, Gogin N, Rinaldi CA, Gill J, Razavi R, Rhode KS Real-time respiratory motion correction for cardiac electrophysiology procedures using image-based coronary sinus catheter tracking., Med Image Comput Comput Assist Interv, 2010;13(Pt 1):391-9